Anomalous phenomena in ECRH experiments at toroidal devices and low-threshold parametric decay instabilities

E.Z. Gusakov[1,2], A.Yu. Popov[1,2], A.N. Saveliev [1,2]

[1]*Ioffe Institute of RAS, St.-Petersburg, Russia*
[2]*RLPAT, St. Petersburg State Polytechnical University, St .Petersburg, Russia*

Electron cyclotron resonance heating (ECRH) at power level of up to 1 MW in a single microwave beam is routinely used in present day tokamak and stellarator experiments and planed for application in ITER. Parametric decay instabilities (PDI) leading to anomalous reflection and/or absorption of microwave power are believed to be deeply suppressed in tokamak megawatt power level electron cyclotron (EC) resonance fundamental harmonic ordinary mode and 2nd harmonic extraordinary mode heating experiments utilizing gyrotrons [1]. Therefore the wave propagation and absorption in these experiments are thought to be well described by linear theory and thus predictable in detail.

However during the last decade a number of observations have been obtained evidencing presence of anomalous phenomena that accompany ECRH experiments at toroidal devices. First of all, non local electron transport was shown to accompany ECRH in some cases indicating that the RF power is not deposited in the regions predicted by standard theory, but is rather redistributed very quickly all over the plasma. Secondly, the first observations of the backscattering signal in the 200 – 600 kW level second harmonic ECRH experiment at Textor tokamak were reported [2] which can be explained in terms of an anomalous backscattering of the EC pump waves. And finally, fast ion generation was observed during ECRH pulse under conditions when energy exchange between electrons and ions should be very low [3, 4].

It is worth noting here that the later two phenomena were observed at the non-monotonic plasma density profile, caused in each specific case by different physical mechanisms such as features of plasma confinement in the magnetic island or electron pump-out effect, originated due to the anomalous convective particle fluxes from the EC layer at the intensive ECRH.

The novel low threshold mechanism of the PDI excitation was proposed in [5] based on analysis of the actual Textor density profile. It was shown that the local maximum of the plasma density, which is usually observed in the O-point of magnetic island at Textor [6], can lead to localisation of the low frequency ion Bernstein (IB) decay wave and thus to suppression of IB wave convective losses in radial direction. A more complicated 2D analysis of the IB wave propagation accounting for the poloidal inhomogenuity of magnetic field in toroidal plasma have shown possibility of IB wave localization in the poloidal direction, as well [7]. The threshold of the backscattering PDI was calculated in this case and shown to be more than four orders of magnitude lower than predictions of standard theory (in the range of 50 kW for the Textor experiment parameters).

Quite recently, the possibility of the IB wave 3D localization and the low-threshold absolute PDI excitation was reported [8]. The analysis performed at fusion relevant parameters for the planned ECRH experiments in JET predicts the threshold of the absolute PDI in the range of 100 kW being approximately four orders of magnitude lower than that predicted by the standard theory [1] and an order of magnitude lower than the threshold of the fast convective PDI. Nevertheless, at low plasma density and temperature the growth rate of this instability appears to be too small to make the instability important for the energy budget. It should be stressed however, that at these plasma parameters another scenario of the low-threshold absolute PDI of the extraordinary mode EC wave, leading to its anomalous absorption via decay into low frequency IB wave and high frequency electron Bernstein (EB) wave, may be realized at the non-monotonic density profile as well. The EB wave in this case is trapped in

the equatorial plane near the density maximum in a 3D toroidal cavity that substantially decreases the threshold of instability, whereas the IB wave propagates to the nearest ion cyclotron harmonic layer and accelerates ions.
In the present paper the experimental conditions leading to the 3D EB wave trapping and substantial reduction of the threshold of the anomalous absorption in ECRH experiments are analyzed. The absolute PDI excitation is predicted and the corresponding threshold is shown to be overcome in the present day experiment.

To elucidate the physics of the absolute PDI we analyze the three wave interaction model in which the extraordinary mode pump wave propagates almost perpendicular to the magnetic field $\vec{H}$ in the density inhomogeneity direction *x* with its polarization vector being mostly directed along the poloidal direction *y*. We represent a wide microwave beam of the extraordinary mode pump wave propagating from the launching antenna inwards plasma along major radius in the tokamak mid-plane as

$$E_{0y} = a_0(y,z)/2 \cdot \exp\left(iq_0 x - i\omega_0 t\right) + \text{ c.c.} \qquad (1)$$

where *c.c.* is complex conjugation, *z* stands for toroidal direction being periodic in tokamak, $a_0 = \sqrt{8\pi / c \cdot P_0 /(\pi w^2)}\exp\left[-(y^2+z^2)/(2w^2)\right]$ is the amplitude, P_0 is the pump wave power and w is the beam waist. The basic set of integral-differential equations describing the decay of the extraordinary mode pumping wave (1) into a daughter IB wave and EB wave: $\vec{E}_I = -\vec{\nabla}\phi_I \exp(i\Omega t)$, $\vec{E}_E = -\vec{\nabla}\phi_E \exp\left(-i(\omega_0 - \Omega)t\right)$, where $\Omega << \omega_0$, is given as:

$$\begin{cases} \hat{D}(\vec{r},\vec{r}';\Omega)\{\phi_I(\vec{r}')\} = 4\pi\rho_I(\vec{r};\Omega) \\ \hat{D}(\vec{r},\vec{r}';\omega_0 - \Omega)\{\phi_E(\vec{r}')\} = 4\pi\rho_E(\vec{r};\omega_0 - \Omega) \end{cases} \qquad (2)$$

The integral operators $\hat{D}$ in (2) are defined in weakly inhomogeneous plasma as follows:

$$\hat{D}(\vec{r},\vec{r}';\omega)\{f(\vec{r}')\} = \int_{-\infty}^{\infty} \frac{d\vec{q}d\vec{r}'}{(2\pi)^3} D\left(\vec{q}, \frac{\vec{r}+\vec{r}'}{2}; \omega\right) \exp\left[i\vec{q}(\vec{r}-\vec{r}')\right] f(\vec{r}'), \qquad (3)$$

where $\omega = [\Omega, \omega_0 - \Omega]$, $D(\vec{q},\vec{r};\omega) = q^2 + \chi_e(\vec{q},\vec{r};\omega) + \chi_i(\vec{q},\vec{r};\omega)$, χ_e and χ_i being defined at a fixed coordinate $\vec{r}$ and consisting of the real and imaginary part are familiar expressions for electron and ion susceptibilities in homogeneous plasmas:

$$\chi_e(\omega_0 - \Omega) = \frac{2\omega_{pe}^2}{\upsilon_{te}^2}\left[1 - \sum_{m=-\infty}^{\infty} \frac{\omega_0 - \Omega}{q_\parallel \upsilon_{te}} Z\left(\frac{\omega_0 - \Omega - m\omega_{ce}}{q_\parallel \upsilon_{te}}\right)\exp\left(-\frac{q_\perp^2\upsilon_{te}^2}{2\omega_{ce}^2}\right) I_m\left(\frac{q_\perp^2\upsilon_{te}^2}{2\omega_{ce}^2}\right)\right] + iq_\perp^2 \frac{\omega_{pe}^2}{\omega_{ce}^3}\nu_{ei};$$

$$\chi_e(\Omega) = \frac{2\omega_{pe}^2}{\upsilon_{te}^2}\left[1 - \frac{\Omega}{q_\parallel \upsilon_{te}} Z\left(\frac{\Omega}{q_\parallel \upsilon_{te}}\right)\exp\left(-\frac{q_\perp^2\upsilon_{te}^2}{2\omega_{ce}^2}\right) I_0\left(\frac{q_\perp^2\upsilon_{te}^2}{2\omega_{ce}^2}\right)\right] - iq_\perp^2 \frac{\omega_{pe}^2}{\omega_{ce}^2}\frac{\nu_{ei}}{\Omega};$$

$$\chi_i(\Omega) = \frac{2\omega_{pi}^2}{\upsilon_{ti}^2}\left[1 - X\left(\frac{\Omega}{q_\perp \upsilon_{ti}}\right) - Y\left(\frac{\Omega}{q_\perp \upsilon_{ti}}\right)\left\{\cot\left(\pi\frac{\Omega}{\omega_{ci}}\right) + \frac{i}{\sqrt{\pi}}\frac{\omega_{ci}}{|q_\parallel|\upsilon_{ti}}\sum_{m=-\infty}^{\infty}\exp\left(-\frac{(\Omega - m\omega_{ci})^2}{q_\parallel^2\upsilon_{ti}^2}\right)\right\}\right];$$

where $q_\perp = |\vec{q}\times\vec{H}|/|H|$, $q_\parallel = \vec{q}\cdot\vec{H}/|H|$ are components of the wave vector, $\vec{H} = |H|\left(\sin\alpha\cdot\vec{e}_y + \cos\alpha\cdot\vec{e}_z\right)$ is an external magnetic field composed of the toroidal and poloidal components, $\sin\alpha = H_y/|H| << 1$, I_m is modified Bessel function of the first kind; and $\chi_i'(\omega_0 - \Omega) << \chi_e'(\omega_0 - \Omega)$; $\xi Z(\xi) = X(\xi) - iY(\xi) = \frac{\xi}{\sqrt{\pi}}\int_{-\infty}^{\infty}\exp(-t^2)\frac{dt}{\xi - t}$ and the nonlinear charge densities $\rho_I(\Omega)$ and $\rho_E(\omega_0 - \Omega)$

$$\rho_I(\Omega) \simeq \chi_i(\Omega)\frac{a_B^*}{8\pi}\frac{\chi_e(\omega_0 - \Omega)\phi_E}{q_\perp^2}, \quad \rho_E(\omega_0 - \Omega) \simeq \chi_e(\omega_0 - \Omega)\frac{a_B}{8\pi}\frac{\chi_i(\Omega)\phi_I}{q_\perp^2}, \qquad (4)$$

where $a_B = E_{0y}/H\cdot\omega_{ce}^2/\left(\omega_0^2 - \omega_{ce}^2\right) \approx E_{0y}/(3H)$.

The PDI threshold decreases substantially when EB wave is trapped at least in x - direction. Which is possible if the turning point of its dispersion curve and the local maximum of the non-monotonous density profile are close one to another. Seeking a solution of the system

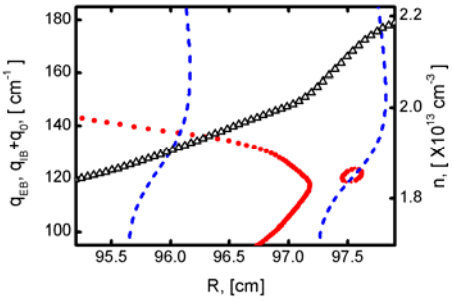

Fig. 1: (a, left and bottom axes): EB (solid lines) and IB (dashed lines) wave 1D dispersion curves (b, right and bottom axes): plasma density (solid line with triangles) versus the coordinate.

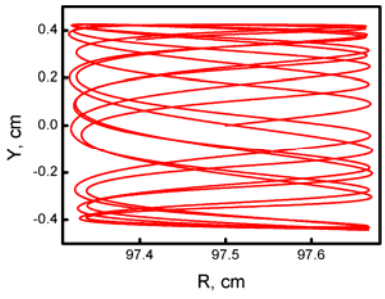

Fig. 2: Trajectory of the EB wave in the poloidal cross – section. $T_e = 1.8\ keV$, $\omega_E / 2\pi = 76.4\ GHz$, $q_E = 118\ cm^{-1}$

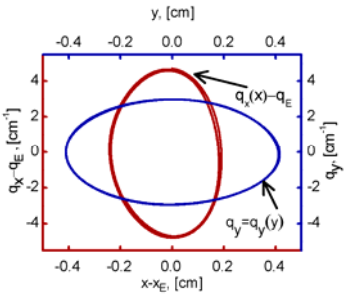

Fig. 3: (Colour on-line) (a, left and bottom axes): The phase portrait $q_x(x) - q_E$; (b, right and top axes): The phase portrait $q_y(y)$;

$\partial^2 D'(\vec{q}, \omega_0 - \Omega, x)/\partial q_x^2 |_E > 0$, $\partial^2 D'(q, \omega_0 - \Omega, x)/\partial x^2 |_E \equiv q_E^2 / L^2 > 0$ hold, provide a global minimum of the dispersion function $D'(q, \omega_E, x)$ over two variables (q, x). This guarantees the existence of two nearby turning points ("warm" to "hot" mode) of the EB wave dispersion curve in plasma and EB wave trapping between them leading to entire suppression of the corresponding convective losses. The trapping of the EB wave is shown in Figure 1 where its dispersion curves at frequency $\omega_{EB} / 2\pi = (\omega_0 - \Omega_I)/2\pi = 76.4\ GHz$ together with the density profile are depicted for the parameters similar to TCV ECRH experiments [4] ($R_0 = 87.5\ cm$, $a = 24\ cm$, $T_e = 1.8\ keV$, $T_i = 350\ eV$, $H(x_m) = 12.6\ kGs$, $n(x_m) = 2.2 \times 10^{13}\ cm^{-3}$, $\omega_0 / 2\pi = 77\ GHz$ and x_m is a position of the density maximum). This figure also illustrates the possibility of three-wave interaction of the EB wave with the 2nd harmonic extraordinary mode pump wave and the IB wave at frequency $\Omega_I / 2\pi = 0.6\ GHz$. The dispersion curve for the latter is shown in Figure 1 up-shifted by the pump wave number $q_0 = 17.2\ cm^{-1}$.

The poloidal dependence of the magnitude of the magnetic field can ensure the localization of the EB wave also in poloidal direction. As it is shown in Figure 2 by the results of the EB wave ray tracing analysis performed accounting for the tokamak equilibria for the same parameters and profiles as used in Figure 1, the ray trajectory is localised in the finite plasma volume. The phase portraits of the motion in radial and poloidal direction are represented by elliptic curves shown in Figure 3 that corresponds to the finite motion. Accordingly, in a vicinity of the turning point of the EB wave $q_x = q_E$, the local maximum of the dispersion function in the radial direction $x = x_E$ (further we will assume $x_E = 0$) and the minimum of the magnetic field in the poloidal direction $y = 0$ the system of integral-differential equation (2) with (3) and (4) reduces to

$$\left\{ iD'_{Iq_x} \frac{\partial}{\partial x} - \frac{\omega_{pe}^2}{\Omega_I^2} \frac{\partial^2}{\partial \xi^2} + iD''_I \right\} b_I = \exp\left[-i \int^x \Delta q dx' \right] \frac{|a_B|}{2} \frac{\chi_i(\Omega_I)\chi_e(\omega_E)}{q_E^2} b_E; \qquad (5)$$

$$\left\{ \hat{D}_E + iD''_E \right\} b_E = \exp\left[i \int^x \Delta q dx' \right] \frac{|a_B|}{2} \frac{\chi_e(\omega_E)\chi_i(\Omega_I)}{q_I^2} b_I \qquad (6)$$

where $b_{I,E}(\vec{r})$ are slowly varying amplitudes of the potentials $\phi_{E,I}(\vec{r})$ defined as $\phi_E(\vec{r}) = b_E(\vec{r}) \exp(iq_E x - i\omega_E t)$, $\phi_I(\vec{r}) = b_I(\vec{r}) \exp\left(i \int^x q_I dx + i\Omega_I t \right)$; $\vec{q}_I = (q_I(x), 0, 0)$ is a solution of the IB wave dispersion relation $D'(\vec{q}_I, \Omega_I, x) = 0$ and $\Omega_I = \omega_0 - \omega_{EB}$; $D'_{Iq_x} = \partial D'(q_I, \Omega_I, x_E)/\partial q_x$; $D''_I = D''(\vec{q}_I, \Omega_I, x_E)$; $\Delta q = q_0 + q_I(x) - q_E$ is a small decay condition mismatch;

$\hat{D}_E = (\omega_{EB} - \omega_E) \left. \frac{\partial D'}{\partial \omega} \right|_E - \left. \frac{\partial^2 D'}{2\partial q_x^2} \right|_E \frac{\partial^2}{\partial x^2} + \frac{q_E^2}{L^2} x^2 + \frac{q_E^2}{q_\xi^2} \frac{\partial^2}{\partial \xi^2} - \frac{q_E^2}{y_0^2} y^2$ $\quad D''_E = D''(q_E, \omega_E, x_E)$; $\quad \varepsilon_m = 1 - m\omega_{ce}/(\omega_0 - \Omega_0)$

$\frac{1}{q_\xi^2}=\frac{\omega_{pe}^2}{q_E^2\omega_0^2}\sum_{m=-\infty}^{\infty}\frac{1}{\varepsilon_m^3}\exp\left(-\frac{q_E^2\upsilon_{te}^2}{2\omega_{ce}^2}\right)I_m\left(\frac{q_E^2\upsilon_{te}^2}{2\omega_{ce}^2}\right)$ $\frac{1}{y_0^2}=\frac{\omega_{pe}^2}{q_E^2\upsilon_{te}^2(x_m-R_0)R_0}\sum_{m=-\infty}^{\infty}\frac{1}{\varepsilon_m^2}\exp\left(-\frac{q_E^2\upsilon_{te}^2}{2\omega_{ce}^2}\right)I_m\left(\frac{q_E^2\upsilon_{te}^2}{2\omega_{ce}^2}\right)$ and coordinates along and across magnetic field on the magnetic surface are introduced by relations $y=\cos\alpha\cdot\eta+\sin\alpha\cdot\xi$, $z=-\sin\alpha\cdot\eta+\cos\alpha\cdot\xi$.

We perform the analysis of the EB wave toroidal cavity parametric excitation using the perturbation theory approach [5] and finally arrive at the following expression valid when the IB wave radial convective losses from the decay region dominate

$$\gamma=-\nu_E+\left.\frac{\partial D_E'}{\partial\omega}\right|_E^{-1}\frac{\chi_e^2(\omega_E)\chi_i^2(\Omega_I)}{4q_E^4D_{Iq_x}'}q_B^2\frac{w^2\delta_x}{\sqrt{w^2+\delta_y^2}}\frac{1}{2R_E} \qquad (7)$$

where $\nu_E=D''|_E\cdot\partial D'/\partial\omega|_E^{-1}$ is the EB wave damping rate, $\delta_x=\sqrt[4]{\partial^2D_E'/(2\partial q_x^2)|_E}\sqrt{L/q_E}$, $\delta_y=\sqrt{\sin\alpha\cdot y_0/q_\xi}$ $J=\frac{\mathrm{Re}}{\sqrt{\pi}}\left\{\int_0^\infty\frac{d\xi}{\sqrt{1-iT\xi}}\exp\left[-\frac{\xi^2}{4}\right]\right\}$, $T=\tau_\perp/\tau_\parallel$ is a coefficient equal to ratio of wave energy convective losses time in radial direction $\tau_\perp=\delta_xD_{I\omega}'/D_{Iq_x}'$ and diffractive loss time along the magnetic field $\tau_\parallel=\Omega^2/\omega_{pe}^2\cdot D_{I\omega}'w^2$.

Dependence of the absolute PDI growth rate on the pump power is shown in Figure 4 for parameters given above resulting in the following PDI characteristics ($q_E=118\ cm^{-1}$, $\delta_x=0.18\ cm$, $\delta_y=0.34\ cm$, $\Omega_I/2\pi=0.6\ GHz$, $\omega_{EB}/2\pi=77GHz$, $\omega_E/2\pi=76.4\ GHz$, $\delta\omega_{0,0}/2\pi=-38\ MHz$).

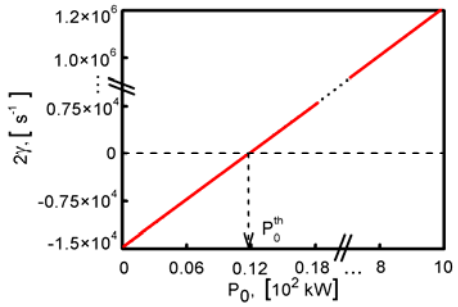

Fig. 4: Growth rate of PDI versus pump power wave for fundamental EB cavity mode.

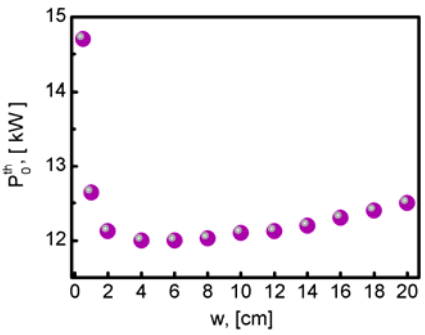

Fig. 5: PDI threshold versus the microwave beam waist.

As is seen, the instability threshold is only 12 kW whereas the growth rate at the power level of 1 MW is high enough ($\gamma\simeq10^6s^{-1}$) to complicate quasi linear instability saturation. Dependence of the PDI threshold pump power on the microwave beam waist obtained from equation (7) is possessing a minimum as shown in Figure 5.

Summarizing we would like to stress the possible role of the low-threshold absolute PDI predicted in this paper in anomalous absorption of microwave power and, in particular, in fast ion production often observed in second harmonic ECRH in toroidal plasmas.

The work supported by RFBR grants 12-02-90003-Bel, 10-02-00887, NWO-RFBR Centre of Excellence on Fusion Physics and Technology (grant 047.018.002), the RAS Presidium program №12 and the RF government grant № 11.G34.31.0041

[1] M. Porkolab et al. Nucl. Fusion, **28** 239 (1988).
[2] E. Westerhof et al. Phys. Rev. Lett., **103** 125001 (2009).
[3] D. Rapisadra et al. Plasma Phys. Control. Fusion, **49** 309 (2007).
[4] A.N. Karpushov et al. in 33rd EPS Conference on Plasma Phys., Rome, ECA, **vol. 30I** P-1.152 (2006).
[5] E.Z. Gusakov et al. Phys. Rev. Lett., 105 115003 (2010).
[6] M. Kantor et al. Plasma Phys. Control. Fusion, **51** 055002 (2009)
[7] E.Z. Gusakov et al. Nucl. Fusion, **51** 073028 (2011).
[8] E.Z. Gusakov et al. JETP Letters, **94** 277 (2011).